Case Studies in Thermal Engineering 28 (2021) 101466

Contents lists available at ScienceDirect

Case Studies in Thermal Engineering

journal homepage: www.elsevier.com/locate/csite

Numerical investigation on the influences of swirling flow to thermal efficiency enhancement of an LPG-energy saving burner

Anirut Matthujak [a,*], Mana Wichangarm [a], Thanarath Sriveerakul [a], Sedthawatt Sucharitpwatskul [b], Sutthisak Phongthanapanich [c]

[a] Combustion and Jet Application Research Laboratory (CJARL), Department of Mechanical Engineering, Faculty of Engineering, Ubon Ratchathani University, Warinchamrap, Ubon Ratchathani, 34190, Thailand

[b] Computer-Aided Engineering Laboratory, Design and Engineering Research Unit, National Metal and Materials Technology Center (MTEC), Pathum Thani, 12120, Thailand

[c] Department of Mechanical Engineering Technology, King Mongkut's University of Technology North Bangkok, Bangsue, Bangkok, 10800, Thailand

GRAPHICAL ABSTRACT

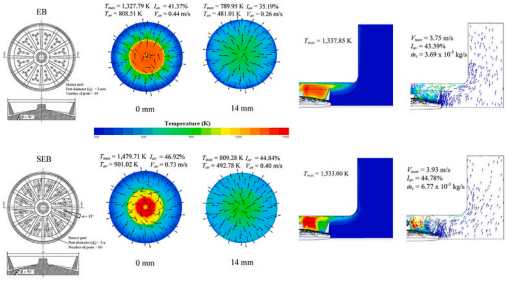

ARTICLE INFO

Keywords:
Swirl energy-saving burner
Thermal efficiency
Heat conversion efficiency
CFD

ABSTRACT

This study investigated a swirling flow in household LPG burners and its effects on thermal efficiency enhancement. Modified from a typical energy-saving burner (EB), a newly invented swirling flame energy-saving burner (SEB) was built and tested both experimentally and numerically. Computational Fluid Dynamics (CFD) simulations were employed to investigate the flow inside the SEB with an inclined angle of 50° and a swirl angle of 15° as well as the flow inside the EB. The computational results were used to calculate the heat conversion efficiencies, which were then compared to the experimental values obtained from the water boiling test (DIN EN 203-2 standard). Additionally, the simulations provide data on the combustion temperature, the turbulence intensity, and the secondary air flow rate. This detailed information clearly confirms

* Corresponding author.
E-mail address: Anirut.m@ubu.ac.th (A. Matthujak).

https://doi.org/10.1016/j.csite.2021.101466
Received 28 May 2021; Received in revised form 7 September 2021; Accepted 15 September 2021
Available online 20 September 2021

that the swirling flow does increase the maximum combustion temperature and the net heat flux into the vessel, directly enhancing the heat conversion efficiency and thus increasing the thermal efficiency. According to the simulations, the heat conversion efficiency of the SEB is around 3.44% greater than that of the EB, while the experiments show that the SEB gives approximately 2.75% higher thermal efficiency than that of the EB. The future expectation is that the heat conversion efficiency can be used to predict the increase in thermal efficiency. With this method, the commercial design of the energy-saving burner can be improved.

Nomenclatures

Symbols

A	Outer surface area of the vessel, m^2
C_p	Specific heat capacity of water, MJ/(kg K)
I	Turbulence intensity, %
m	Mass of the water in the pot, kg
$\dot{m}$	Mass flow rate, kg/s
Q	Lower heating value of LPG, *107.7*MJ/m^3
q''	Average net heat flux gained at the vessel, kW/m^2
T	Temperature, °C, K
Δt	Time interval used to boil the water from T_{w1} to reach T_{w2}, s
$\dot{V}$	LPG volume flow rate at each LPG released pressure, m^3/s
V	Velocity, m/s

Greek Symbols

α	Swirl angle
β	Inclined angle
η_{th}	Thermal efficiency
η_h	Heat conversion efficiency

Abbreviations

CB	Conventional LPG cooking burner
CFD	Computational Fluid Dynamics
EB	Energy-saving burner
SEB	Swirling flame energy-saving burner
LPG	Liquified Petroleum Gas

Subscripts

w1	Initial state of water
w2	Final state of water
av	Average
max	Maximum
s	Secondary air
f	LPG as fuel
EB	Energy-saving burner
SEB	Swirling flame energy-saving burner

1. Introduction

LPG cooking burners are widely used for domestic heating because of their safety and ease of use. The central subject of numerous studies was enhancing the thermal efficiency of a conventional LPG cooking burner (CB). Among these was the introduction of an LPG energy-saving burner (EB) in Thailand [1]. In general, an EB produced stronger combustion than that from a CB. The former could achieve around 40% thermal efficiency in the water boiling test (DIN EN 203-2 standard [2]), while the latter could only reach approximately 35% thermal efficiency [3]. Furthermore, many pieces of evidence suggested that the thermal efficiency of EBs could be further improved according to the second law of thermodynamics. As reviewed by Datta et al. [4], the techniques that have been frequently used to improve the thermal efficiency of LPG burners are for example, improving geometrical design, enhancing mixing of air-fuel, heat recirculation using porous medium, applying the swirl flow.

Aroonjarattham [5] investigated the geometrical design of the holes on both the outer and the inner rings of the burner cap of the

LPG cooking burners. More specifically, the effects of the hole angles and the number of holes on the thermal efficiency were studied. Aroonjarattham reported that the thermal efficiency was increased by 13% when the outer ring hole angle was 75°, by 2% when the inner ring hole angle was 60°, by 5% when the number of the outer ring holes was 50, and by 7% when the number of the outer ring holes was 20.

Chaelek et al. [6] proposes a design of an atmospheric gas burner with heat recirculation combustion by applying porous media combustion technology. The results show that, the burner with firing rates from 21 to 44 kW resulted in evaluated air temperatures of 136–252 °C, yielding maximal temperatures greater than the adiabatic flame temperature.

Based on the design concept of radial flow slotted burners, most CBs and EBs feature open combustion flames and lose a large amount of energy to the surroundings, resulting in low thermal efficiency [3]. To minimize the heat loss due to the open flame, a swirl burner (SB) featuring a swirling flame was introduced and investigated. Shtern et al. [7] showed analytically that a swirling jet improved heat and mass transfer rates significantly. The swirling flame utilized rotational flow motion to efficiently mix the hot gas with the surrounding air and prolong the residence time [8–14]. In 1989, Tamir et al. [8] published experimental research in which they designed and built an SB. In their burner, the burner ports were aligned with an inclined angle (β) of 26° and with a swirl angle (α) of 15° to produce the swirling central flame. The combination of these two angles forced the combustion flame to swirl at the center of the burner cap. As a result, their burner provided a 6% increase in the thermal efficiency from the CB. An explanation for the increase was that the high shear stress in the rotating movement flow resulted in the following advantages: (1) air-fuel mixing enhancement due to prolonged mixing time, (2) heat transfer amplification due to longer residence time and increase in the area between the flame and the vessel surface, and (3) combustion improvement due to additional secondary air entrainment. The thermal efficiency of an SB can be affected by many parameters, including the gas-flow rate, the swirl angle, and the number of burner ports. Based on the work done

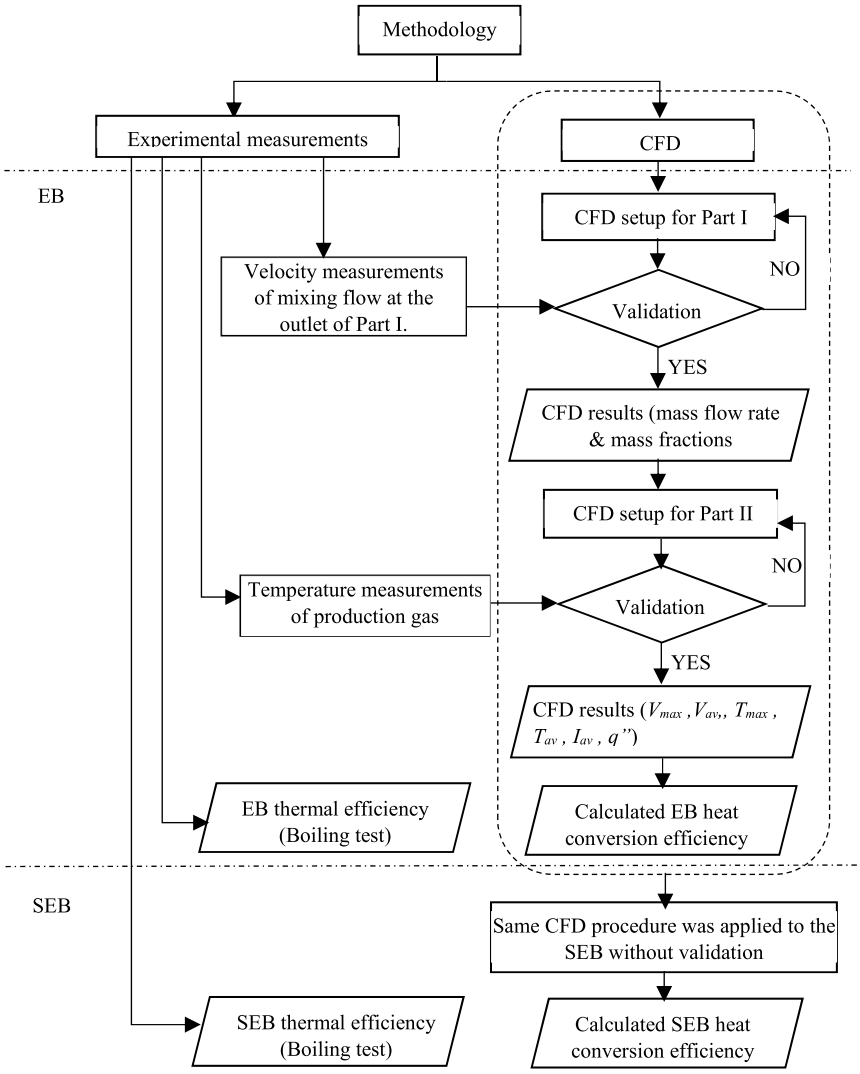

Fig. 1. Flowchart of the research methodology in this work.

by Tamir et al. [8], Jugjai et al. [9] studied the heat transfer mechanism of the SB with modification to the number of burner ports. Their experiment showed that the thermal efficiency of the SB was 15% greater than that of the CB due to its higher heat transfer coefficient between the hot gas and the vessel surface. Another experimental investigation of an SB was done by Hou et al. [10]. Five parameters, including some related to the swirling flow, were found to affect the thermal efficiency and the CO emission. The results indicated that the SB gave 12% higher thermal efficiency and lowered CO emission than the CB. Basu et al. [11] investigated the combustion and the emission characteristics of the LPG cooking burners commonly used in India. Various modifications in the burner cap and fuel injection nozzles were investigated experimentally. It was found that orienting the ports to generate a swirling flow increased the thermal efficiency by 3% while also decreasing the emission significantly. Zhen et al. [12] reported that the swirling flow had been successfully induced in many industrial applications. In their work, two domestic SBs were designed with two different methods to generate a swirling motion. The two burners were then experimentally compared to another burner for benchmarking. The results showed that, under certain operating conditions, the SBs had higher heating efficiency and lower CO emission than those of the benchmarking burner. Kotb and Saad [13] reported a comparative experimental investigation between a co-swirl burner, a

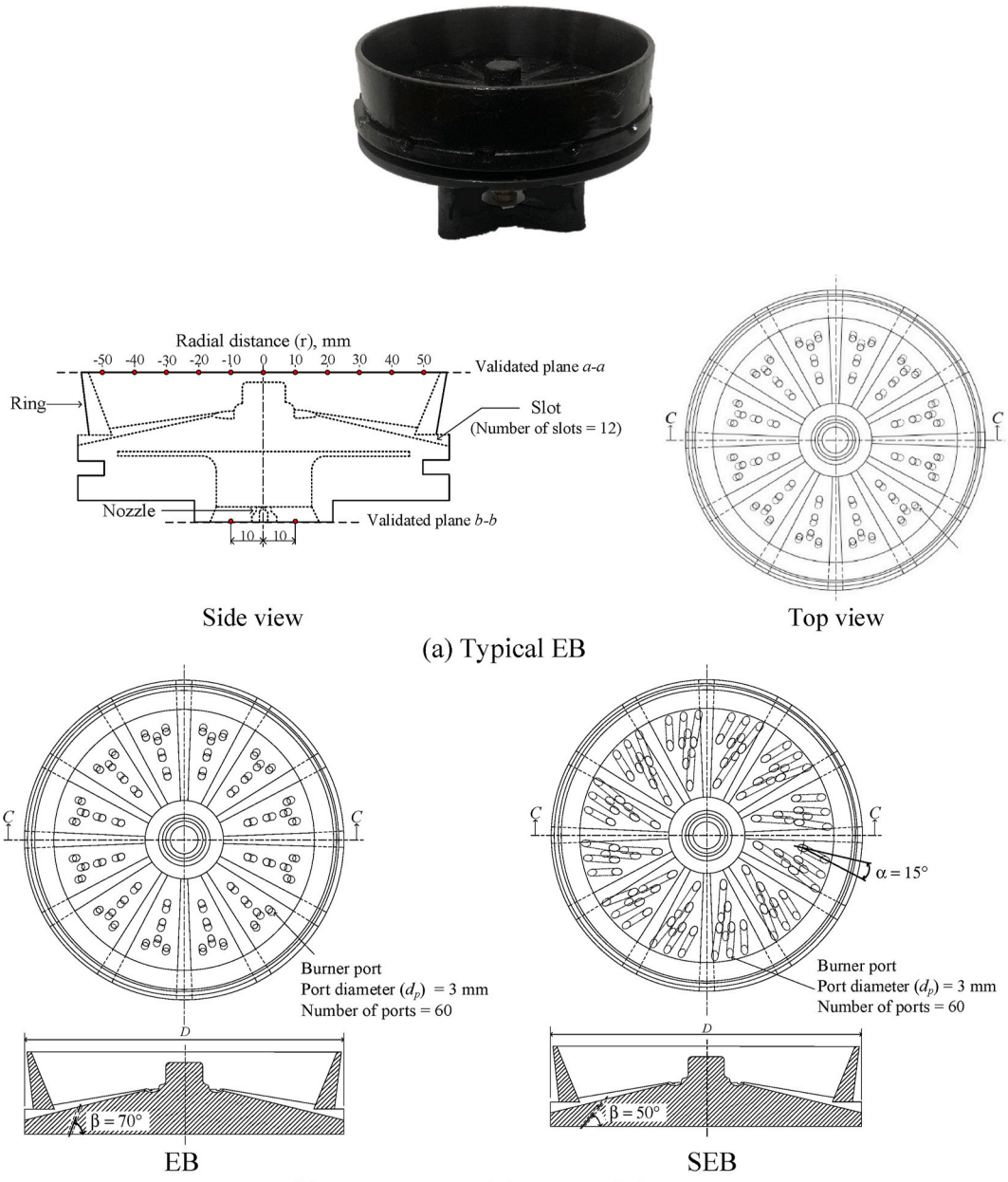

Fig. 2. Schematic diagrams of the EB and SEB.

counter-swirl burner, and a conventional domestic (non-swirl) burner. The results indicated that the thermal efficiencies (under all operating conditions) of both the co-swirl and the counter-swirl burners were higher than that of the non-swirl burner. For example, at Reynolds number of 2000 and equivalence ratio of 1, the thermal efficiencies of the co-swirl and the counter-swirl burners were 8.8% and 5.8% higher than that of the non-swirl burner, respectively. The co-swirl and the counter-swirl burners also released less CO gas than the non-swirl burner. Moustafa et al. [14] studied the swirling effect on a single ring gas domestic burner. The results indicated that, using the swirl motion improved the thermal efficiency and CO emissions. For the Swirl flow burner, the efficiency increased by 2.7% from the benchmarked burner. On the other hand, the CO emission decreased by 80%. Hou and Chou [15] the effects of swirl angle and inclination angle on the performance of the swirl flow burner. A greater swirl angle results in higher thermal efficiency and CO emission. For a lower loading height, the highest efficiency occurs at the inclination angle 15°. On the other hand, at a higher loading height, thermal efficiency increases with the inclination angle.

In many past studies, combustion analysis of the SBs was limited to measurements and observations. Extensive experiments typically investigated the effects of the swirling flow on thermal efficiency. Explanations of why the swirling flow enhanced the thermal efficiency were mainly based on qualitative observations. Although Jugjai et al. [9] attempted to explain the thermal efficiency enhancement by using the quantitative measurement of the heat transfer coefficient at the vessel surface, a clear insight into what specific features of the swirling flow led to the higher thermal efficiency could not be shown from the experimental evidence.

Nowadays, computer simulation is indispensable for analyzing and improving reacting flow systems [16–26]. A few studies (e.g., Boggavarapu et al. [25] and Francisco et al. [26]) employed CFD simulations to predict the combustion and the heat transfer in the cooking burners; however, most of them focused on burners without a swirling flow. The purpose of this study is to investigate a newly invented swirling flame energy-saving burner (SEB). The SEB is a typical energy-saving burner (EB) with modifications to include a swirling flow. CFD simulations were performed and used to clearly explain why the SEB has higher thermal efficiency than that of the (non-swirl) EB. The numerical data include the secondary air flow rate, average turbulence intensity, the maximum combustion temperature, the temperature profile, the maximum velocity, and the heat flux. These quantitative results provide an insight to better understand the increase in the efficiencies and confirm that a swirling flow with high shear stress does indeed result in the thermal efficiency enhancement of the SEB, as described by Tamir et al. [8].

The research methodology of this study is shown in Fig. 1.

1.1. Experiment

1.1.1. The burners

Fig. 2 illustrates the burners used in this study: the typical EB [27] and the SEB. The measurement points for temperature and velocity in the *a-a* and *b-b* planes are marked as red dots in Fig. 2(a). Unlike the CB, the EB and the SEB have no mixing tube. The EB and the SEB have almost identical geometry except for the orientation of the burner ports on the burner cap (Fig. 2(b)). Currently available in Thailand's market, the (non-swirl) EB has its burner ports oriented with an inclined angle of 70° and a swirl angle of 0°. On the other hand, the burner ports of the SEB are oriented with an inclined angle of 50° and a swirl angle of 15° as shown. According to Tamir et al. [8], the best inclined angle of 26° and the swirl angle of 15° could provide the highest thermal efficiency (for the SB); however, due to the geometrical limitation of the burner cap in this study, the inclined angle of 50° was used instead for the SEB.

1.1.2. Thermal efficiency test

The thermal efficiencies of both the EB and the SEB were measured to quantify the thermal efficiency enhancement due to the swirling flow. The water boiling test was conducted for both the EB and the SEB. Measured temperature and velocity of the hot gas at the specified points (Fig. 2(a)) would be later used to validate the CFD models. Following the water boiling test of the DIN EN 203-2

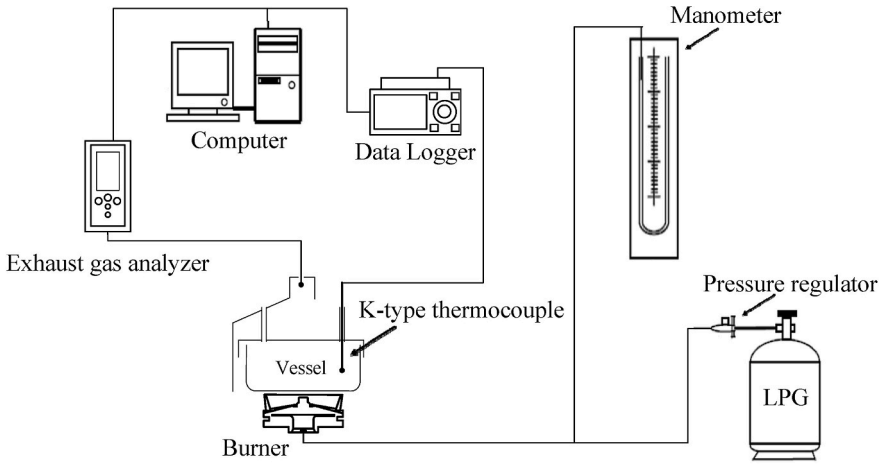

Fig. 3. Setup of the thermal efficiency test.

standard [2], the experimental equipment was set up as shown in Fig. 3. After the LPG flow rate ($\dot{V}$) had been regulated to the desired value, and the burners were preheated for 15 min. A 26-cm-diameter cooking pot contained 6.1 kg of water (m) with known temperature (T_{w1}) was then placed on top of the burner. Immediately after the plot had been placed, water temperature and time were recorded until the water temperature inside the pot reached 90 °C (T_{w2}). A U-tube manometer used to regulate the LPG flow rate had a resolution of 1 mm with an uncertainty of 0.5 mm. The K-type thermocouple with an uncertainty of ±1.1 °C was used to measure the water temperature.

The thermal efficiency (η_{th}) can be calculated by

$$\eta_{th} = \frac{mC_p(T_{w2} - T_{w1})}{\dot{V}Q\Delta t} \times 100, \tag{1}$$

where C_p is the specific heat capacity of water, and Δt is the time duration used to heat the water from its initial temperature to 90 °C. Every test case was repeated three times and ensure the accuracy of the data.

2. Numerical simulation

The main objective of this research is to utilize CFD simulations as a tool to investigate and gain an insight into the flow and the combustion inside the SEB and the ES. ANSYS FLUENT version 15.0, a commercial CFD software application was used. The evaluation of the thermal efficiency of the cooking burner from any testing standard is always based on some boiling test over a time interval, which is a transient heat transfer problem. The transient heat transfer is rather complicated and requires substantial hardware resources and computational time to simulate using CFD. Therefore, this research used a steady-state 3D model with a specified temperature at the outer surface of the pot to simplify the problem with a certain degree of compromised accuracy.

Moreover, to reduce the complexity of the geometric domain and the numerical scheme, the numerical domain was divided into two parts, as shown in Fig. 4(a).

In Part I, mixing flow phenomena between the LPG and the air was simulated without combustion (cold test simulation). The same geometric domain was applied for both the EB and the SEB for the Part I model. The mesh for Part I was discretized into tetrahedral elements, as shown in Fig. 4(b1). An adiabatic (zero heat flux), non-slip wall condition was set at the burner cap and the ring wall. A pressure inlet condition at 1 atm and 300 K was set at both the fuel and the air inlets. The top of the burner cap was set as a pressure outlet, as shown in Fig. 4(b2). The RNG k-ε turbulence model was selected to determine the turbulence characteristics inside these high-pressure burners. The high-speed LPG flow mixed with the low-speed entrained air flow in this region, so the RNG k-ε turbulence

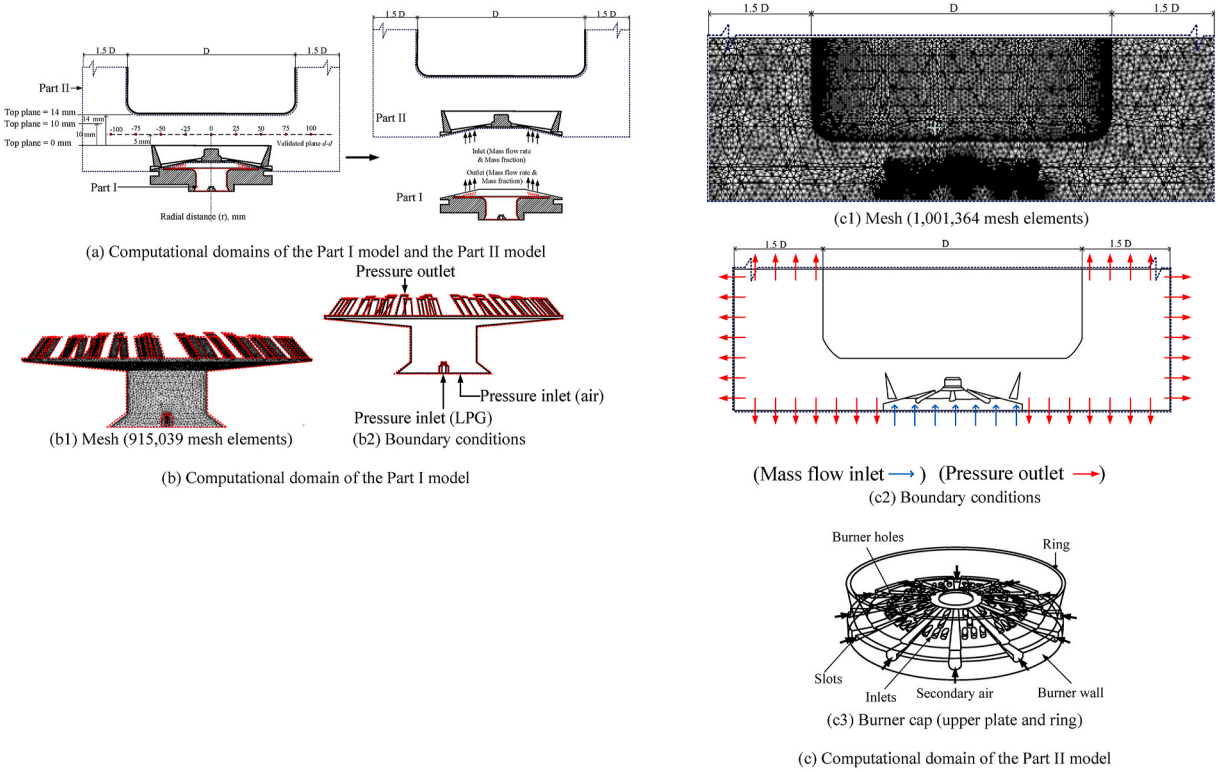

(a) Computational domains of the Part I model and the Part II model

(b1) Mesh (915,039 mesh elements)

(b2) Boundary conditions

(b) Computational domain of the Part I model

(c1) Mesh (1,001,364 mesh elements)

(c2) Boundary conditions

(c3) Burner cap (upper plate and ring)

(c) Computational domain of the Part II model

Fig. 4. (cont.). The computational domain.

model was a good choice since it could account for wide ranges of speeds and Reynolds numbers [28,29]. The species transport model was also enabled to simulate the air-fuel mixing. The LPG contained 50% propane and 50% butane by weight. Gravitational and buoyancy effects were also considered in the simulation. The model setup and the boundary conditions for this cold test simulation are listed in Table 1. The solutions obtained from this simulation, including the mixing mass flow rate and species mass fractions (propane, butane, oxygen, and nitrogen), would later be used as input data for Part II.

In Part II, combustion reaction and heat transfer models must also be used (hot test simulation). The geometric domain spanned from the top of the burner cap to the zone adjacent to the pot surface. The domain diameter was extended to four times the pot's diameter, as shown in Fig. 4(c2) to minimize the effect of the physical free boundary condition. The domain was discretized with a tetrahedral mesh, as shown in Fig. 4(c1). A mass flow inlet condition with species mass fractions obtained from Part I (different for each LPG pressure) was applied, as illustrated in Fig. 4(c2). The opening slots for entraining the secondary air were set as pressure inlets at 1 atm (Fig. 4(c3)). The thermal resistance of the vessel wall was neglected to minimize the complexity of fluid-solid interaction. The amount of the net heat flux at the outer surface of the vessel would be used to calculate the heat conversion efficiency defined below. The heat transfer in consideration was mainly from the heat convection due to the hot flue gases (i.e., products of the combustion) and the heat radiation from the flame. The standard k-ε turbulence model was applied, as done by Boggavarapu et al. [25], where the combustion took place, and most of the LPG and the air contents were already mixed due to the high Reynolds number flow [30–32]. Eddy dissipation combustion model was also selected. The Discrete Ordinates (DO) radiation model was applied to account for a potentially significant difference in combustion temperature. The same radiative heat transfer model was also implemented by Boggavarapu et al. [25]. The convergence criterion for the computational residuals was set at 10^{-6}. Table 2 summarizes the model setup and boundary conditions for Part II.

Since the simulation was steady-state, the computational results could not be used to compute the thermal efficiency directly. This research introduces a newly defined efficiency called heat conversion efficiency (η_h). It is defined as the ratio of the heat flux at the vessel (representing the energy reaching the vessel) to the energy supplied by the burner. The heat conversion efficiency can be calculated as follows:

$$\eta_h = \frac{q''A}{\dot{m}_f Q}, \tag{2}$$

where q'' is the average net heat flux at the vessel surface (kW/m^2), A is the outer surface area of the vessel (m^2), $\dot{m}_f$ is the mass flow rate of the LPG obtained from the CFD simulation (kg/s), and Q is the lower heating value of the LPG (kJ/kg).

3. Results and discussions

3.1. Validation

The CFD calculations were considered as converged when the two following criteria were met. The first condition was that the computational residuals were lower than 10^{-6}. The other required that the difference between the total mass fluxes entering and leaving the domain was smaller than 10^{-7} so that the principle of mass conservation was sufficiently observed. In addition, the validation against the experimental data for both parts was conducted for the EB to ensure that the model was sufficiently accurate.

For Part I, the mixing flow velocity distribution was validated against the experimental measurements at the LPG released pressure of 0.2 bar. As shown in Fig. 2(a), eleven measuring points were located above the burner ring at the upper *a*-*a* plane and were 10 mm apart along the radial direction. At the lower *b*-*b* plane, there were two more measuring points for measuring the velocity of the induced primary air. The flow velocities were measured using hot-wire anemometers (Testo-435 model) with an uncertainty of ±0.03 m/s (±5% error of reading). It was found that the velocity values from the CFD simulation and the experimental data agreed with a maximum error of 3.27% at the upper plane and with a maximum error of 6.98% at the lower plane.

For Part II, the temperature result from the simulation was validated against the experimental data at the specified *d*-*d* plane as shown in Fig. 4(a). This comparison was also done at the LPG released pressure of 0.2 bar. *K*-type thermocouples with a data logger with an uncertainty of ±1.1 °C (±0.4% error of reading) were used to measure the water temperature. The maximum discrepancy was less than 5.75%.

Table 1
Model setup and boundary conditions for Part I.

Boundary Conditions and Models	Selected Values
Inlet Boundary Conditions	Air Inlet Gauge Pressure = 0 Pa LPG Inlet Gauge Pressure = 20,000 Pa
Outlet Boundary Condition	Pressure Outlet (Air Outlet Gauge Pressure = 0 Pa)
Solver Type	Pressure-based
Time	Steady-state
Near-wall Treatment Method	Standard Wall Function
Turbulence Model	RNG k-ε Model
Other Model(s)	Species Transport
Propane: Butane	50 : 50
Operating Condition	Operating Pressure = 1 atm

Table 2
Model setup and boundary conditions for Part II.

Boundary Conditions and Models	Selected Values
Inlet Boundary Conditions	Mass Flow Inlet (from Part I) Mass Fractions of C_3H_8, C_4H_{10}, N_2, and O_2 (from Part I) Air Inlet Gauge Pressure = 0 Pa
Outlet Boundary Condition	Pressure Outlet (Air Outlet Gauge Pressure = 0 Pa)
Solver Type	Pressure-based
Time	Steady-state
Near-wall Treatment Method	None
Turbulence Model	Standard k-ε Model
Radiation Model	Discrete Ordinates (DO) Radiation Model
Combustion Model	Eddy Dissipation Model
Operating Condition	Operating Pressure = 1 atm

From the validation results, it may be concluded that the CFD models can be used to investigate the flow detail for the EB accurately. Thus, predicting the flow and combustion results for the SEB with the same CFD methodology should be equally valid.

3.2. CFD results

This section discusses the effects of the LPG released pressure on the flow field and the combustion temperature distribution obtained from the CFD results. As previously mentioned, the geometries of the EB and the SEB were identical except for the orientation of the burner ports. Since the mixing mass flow rate and the species mass fractions from Part I were used as inputs for Part II, only the results from the latter are presented and discussed here. Fig. 5 shows the contour plots of the temperature distributions and the vector plots of the velocity fields on the midplane at the LPG pressures of 0.2 and 1.0 bar. At the other simulated LPG pressures, selected flow quantities were reported in Table 3. At the same LPG pressure, the SEB produced the high-temperature zone more tightly concentrated around the center of the burner cap, while that of the EB was more spread out. The tightening of the high-temperature zone was due to the swirling flow caused by the burner ports with 50° inclined angle and 15° swirl angle. The velocity vector plots (Fig. 5) showed that the entrained secondary air of the SEB circulated near the ring region, effectively preventing the high-temperature zone from spreading away from the center. When operated at a higher LPG released pressure, the EB produced a combustion flame (or the high-temperature zone) that was more forcefully spread out of the ring region. Thus, a larger surface area of the pot was in contact with the flame. On the other hand, the combustion flame of the SEB still mainly remained inside the ring region. Its high-temperature zone outside the ring region was relatively thin and close to the solid surface. The broader high-temperature zone of the EB resulted in the higher heat loss, while the SEB featured the swirling flow that tightened the high-temperature zone as a mechanism to reduce the heat loss from the hot gas flow.

Fig. 6(a) shows the comparison between the EB and the SEB in terms of the average turbulence intensity (I_{av}) and the secondary air flow rate ($\dot{m}_s$) at the midplane. The average turbulence intensity rose with the increasing LPG pressure. The SEB provided a higher average turbulence intensity and a higher secondary air flow rate at all LPG pressures than those of the EB. The combustion was evidently enhanced not only by a higher air-fuel mixing quality (due to more intense fluid velocity fluctuation) but also by a better air-fuel ratio. This also confirmed the advantage of the SB as reported in Tamir et al. [8].

Fig. 6(b) shows the comparison between the two burners in terms of the maximum temperature and the maximum velocity at the midplane. The maximum temperature and the maximum velocity of the SEB were higher than those of the EB by 14.08%, and 46.86% on average, respectively. The SEB also produced a flame jet that was more impinging on the solid surface (see Fig. 5), generating a tremendous heat transfer rate to the vessel. Consequently, the maximum temperature from the SEB varied only in a narrow range of 1,533 K to 1,549 K (ΔT_{max} = 16K), while the range from the EB was 1337.55 K–1368.43 K (ΔT_{max} = 30.58K). It may be concluded that the SEB provides a higher and more stable maximum temperature. It is worth noting that the combustion in cooking burners is usually a combination of mainly premixed combustion and partly diffusion combustion [33] and that both of the burners have almost the same rates of increase in the maximum temperature and the maximum velocity as the LPG pressure increases.

Fig. 7 and Table 4 show the temperature and the velocity distributions at three specified horizontal planes located at 0, 10, and 14 mm above the burner ring (see Fig. 3(a)). The improvement of the SEB over the EB could be clearly observed. The hot temperature zone of the SEB (above 1,200 K) was forced to concentrate around the center of the burner, while the hot temperature zone of the EB (900–1,200 K) was more dissipated outward.

On the first plane (at the burner ring level), at the LPG released pressure of 0.2 bar, the maximum temperature of the SEB (1497.71 K) was higher than that of the EB (1327.79 K), as shown in Fig. 7(a1). This was caused by the swirling flow, or a stronger flow rotation motion, as indicated by the directions of the velocity vectors in the figure. At a higher LPG pressure, the advantage of the swirling flow still existed, but the differences in the maximum temperature and the average turbulence intensity were smaller. When averaged over the considered pressure range, the temperature and the turbulence intensity of the SEB were higher than those of the EB by around 12.59% and 10.04%, respectively (see Fig. 7(a1)-(e1)).

On the second plane (10 mm above the burner ring and 4 mm below the vessel), the rotation of the swirling flow still provided stronger combustion for the SEB; however, its influence was partially overcome by the radial diffusion of the flame, resulting in the decrease of the maximum temperature. When averaged over the considered pressure range, the temperature and the turbulence

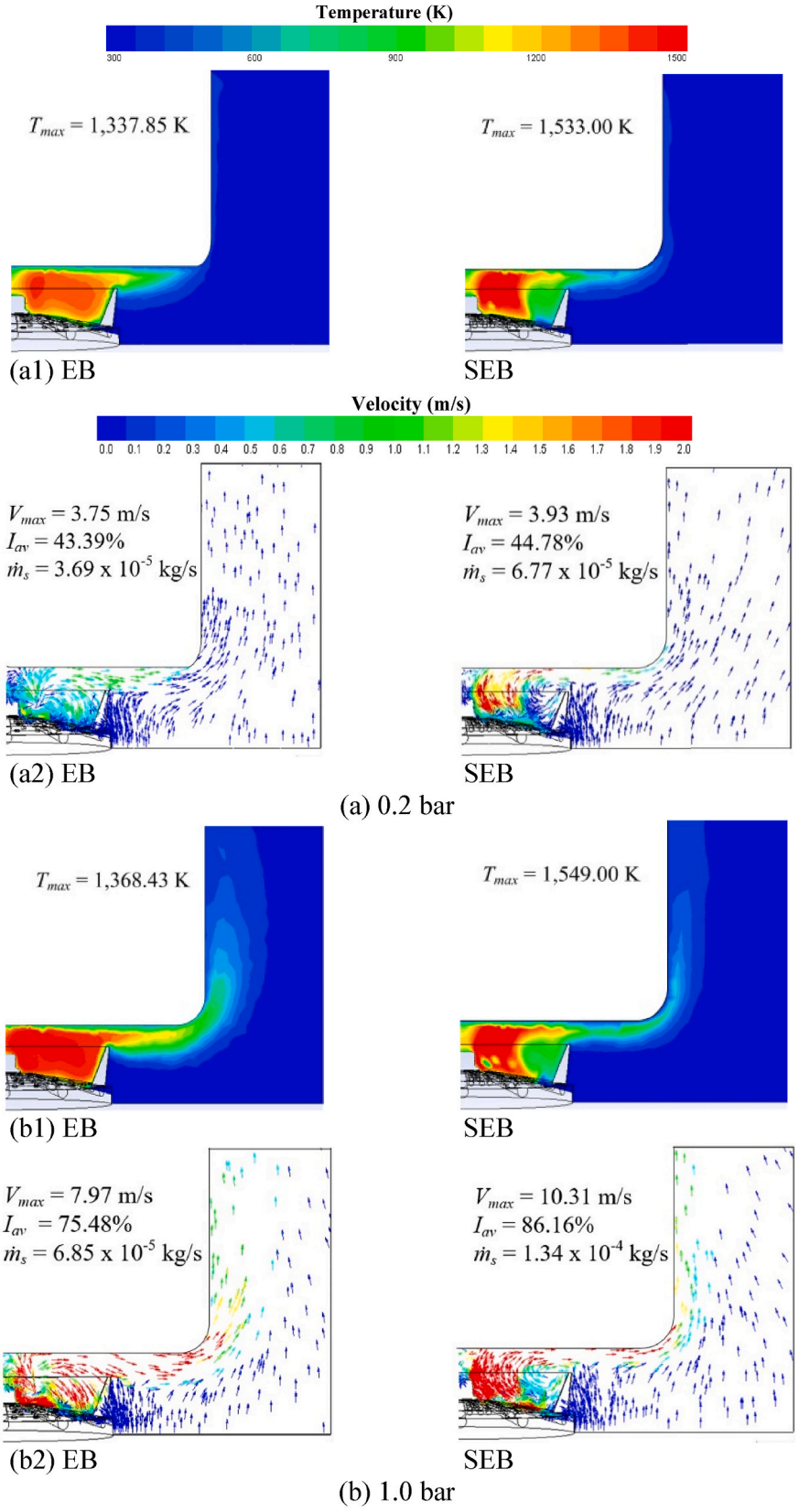

Fig. 5. The temperature and the velocity distributions at two different LPG pressures (midplane view).

Table 3
Report of selected flow quantities on the midplane at various LPG pressures.

LPG (bar)	Burner	T_{max} (K)	T_{av} (K)	V_{max} (m/s)	V_{av} (m/s)	I_{av} (%)	$\dot{m}_s$ x 10^{-5} (kg/s)
0.20	EB	1337.85	812.80	3.75	0.45	43.39	3.69
	SEB	1533.00	933.47	3.93	0.76	44.78	6.77
0.40	EB	1345.67	818.09	5.17	0.61	53.68	4.68
	SEB	1539.00	937.12	7.62	0.92	59.84	7.70
0.60	EB	1355.71	824.36	6.30	0.74	62.47	5.93
	SEB	1542.39	938.58	8.75	1.09	69.96	10.10
0.80	EB	1361.17	827.33	7.29	0.86	67.51	6.39
	SEB	1546.60	940.53	9.83	1.18	78.46	11.90
1.00	EB	1368.43	831.29	7.97	0.94	75.48	6.85
	SEB	1549.00	943.22	10.31	1.24	86.16	13.40

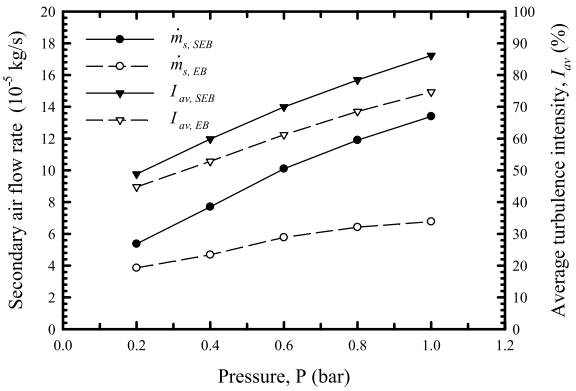

(a) The average turbulence intensity and the secondary air flow rate

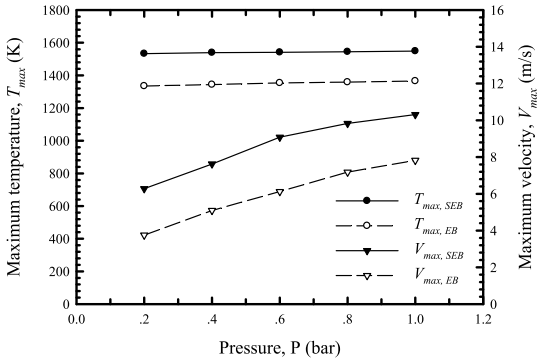

(b) The maximum temperature and the maximum velocity

Fig. 6. Comparison of the EB and the SEB at the midplane.

intensity of the SEB were higher than those of the EB by around 13.80% and 33.42%, respectively (see Fig. 7(a2)-(e2)).

Lastly, on the third plane (immediately beneath the vessel), at the pressure of 0.2 bar, the influence of the swirling flow was the smallest. The radial diffusion of the flame was more effective and caused the loss of kinetic energy, drastically decreasing the maximum temperature. There was no significant difference in the maximum temperature (around 3%) between the two burners.

It can be concluded that the swirling flow plays an essential role in blocking the flame and forcing it to flow around the center of the burner. The air-fuel mixing is then promoted by the increase in the average turbulence intensity, resulting in a higher maximum flame temperature. The advantages of the SEB can be clearly seen numerically and experimentally.

In summary, the CFD results illustrate that the swirling central flame exists for the SEB. As mentioned before, the swirling flame utilizes the rotational flow motion to enhance the mixing of the hot gas with the surrounding air and to prolong the residence time [8–15]. This swirling central flame increases the turbulence intensity and the amount of entrained secondary air and the maximum temperature and the maximum velocity. Increases in these parameters result in a higher heat flux gained at the vessel and, hence, the higher thermal efficiency, as discussed in the next section.

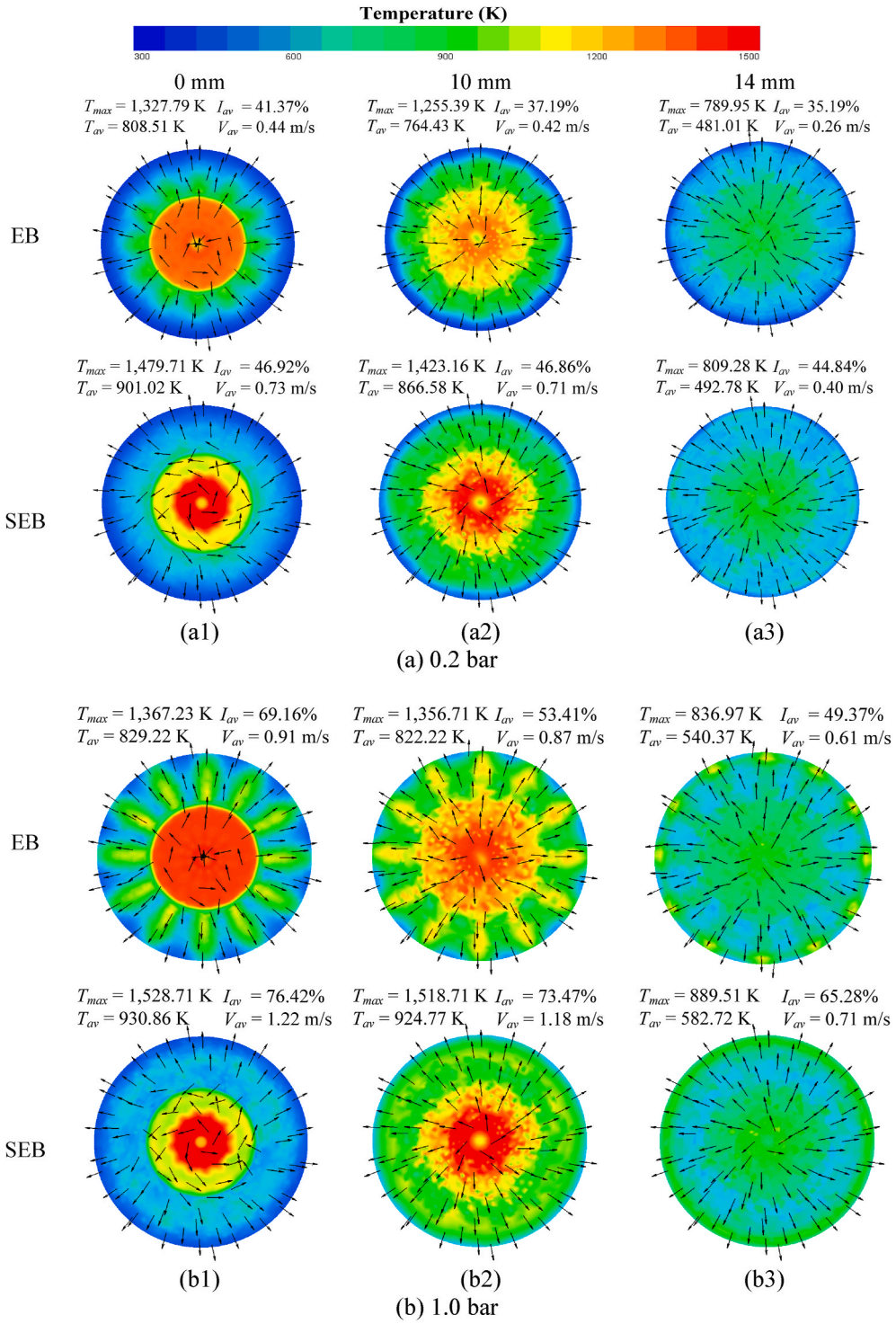

Fig. 7. The temperature and the velocity distributions at three specified horizontal planes at two different LPG pressures.

3.3. Heat conversion efficiency and thermal efficiency

Fig. 8 compares the net heat fluxes, the heat conversion efficiencies, and the thermal efficiencies between the two burners at five different LPG released pressures. Recall that the CFD software directly computed the net heat flux (q'') at each LPG released pressure, and the heat conversion efficiency (η_h) was then determined using Eq. (2). In contrast, the thermal efficiency (η_{th}) was calculated from

Table 4
Report of selected flow quantities on the three specified planes at various LPG pressures.

LPG (bar)	Burner	0 mm				10 mm				14 mm			
		T_{max} (K)	T_{av} (K)	I_{av} (%)	V_{av} (m/s)	T_{max} (K)	T_{av} (K)	I_{av} (%)	V_{av} (m/s)	T_{max} (K)	T_{av} (K)	I_{av} (%)	V_{av} (m/s)
0.20	**EB**	1327.79	808.51	41.37	0.44	1255.39	764.43	37.19	0.42	789.95	481.01	35.19	0.26
	SEB	1479.71	901.02	46.92	0.73	1423.16	866.58	46.86	0.71	809.28	492.78	44.84	0.40
0.40	**EB**	1345.16	817.82	50.03	0.59	1290.95	785.60	41.83	0.56	807.82	489.82	39.07	0.34
	SEB	1514.05	921.93	53.56	0.85	1478.89	900.52	53.07	0.85	828.16	504.28	49.93	0.47
0.60	**EB**	1355.21	820.18	57.32	0.73	1314.51	800.42	46.27	0.68	822.42	505.16	43.24	0.46
	SEB	1525.71	929.03	61.84	1.05	1501.45	914.26	60.43	0.98	849.67	517.38	54.03	0.60
0.80	**EB**	1360.95	825.50	61.43	0.84	1327.16	804.99	48.03	0.76	830.72	503.30	44.42	0.56
	SEB	1527.49	928.91	68.91	1.12	1512.36	919.71	66.73	0.97	868.77	527.85	60.93	0.66
1.00	**EB**	1367.23	829.22	69.16	0.91	1356.71	822.22	53.41	0.87	836.97	540.37	49.37	0.61
	SEB	1528.71	930.86	76.42	1.22	1518.71	924.77	73.47	1.18	889.51	582.72	65.29	0.71

the experimental data using Eq. (1).

A higher LPG pressure results in higher net heat flux, as one intuitively expects. In contrast, the heat conversion and the thermal efficiencies decrease with the increasing pressure, as shown in Fig. 8. This is due to the rise in heat loss when the pressure increases. The decreasing trend of the thermal efficiency as the LPG pressure increased is a well-known behavior of the LPG cooking burners explained by many researchers [3,5,9,10]. According to Fig. 8, the SEB has a higher thermal efficiency than that of the EB at all pressure levels. The highest thermal efficiency of the SEB is around 50% (according to DIN EN 203-2 standard) at the LPG pressure of 0.2 bar. This value is 3.95% higher than the highest thermal efficiency of the EB and 11.76% higher than that of the CB [27]. When averaged over the entire test pressure range, the thermal efficiency of the SEB is 44.49%, which is 2.75% higher than that of the EB (41.74%). The increase in the average thermal efficiency due to a swirling flow was reported to be around 6% by Tamir et al. [8]. The smaller increase in the current study can be explained by the differences in the inclined and the swirl angles.

The trend of the heat conversion efficiency is very similar to the trend of the thermal efficiency, except that the heat conversion efficiency is always smaller than the thermal efficiency at the same LPG pressure (because the heat conversion efficiency only takes into account the steady-state heat transfer into the wetted area). According to Fig. 8, the average heat conversion efficiency of the SEB is 17.60% which is 3.44% higher than that of the EB (14.16%). Over the simulated pressure range, the CFD results predict the heat conversion efficiency of the SEB to be, on average, 3.44% greater than that of the EB. Also, the experiment confirms that the thermal efficiency of the SEB is, on average, 2.75% higher than that of the EB. Therefore, the average increment in the simulated heat conversion efficiency is 0.70% higher than the average increment in the experimental thermal efficiency. Due to the concordance between the definitions of the two efficiencies (as the ratio of a heat sink to the heat input), it is reasonable to expect that the increment in the heat conversion efficiency can be used to estimate the increment in the thermal efficiency.

According to the 2030 Agenda for Sustainable Development adopted by the United Nations in 2015 [34], the results of this study could help to accomplish two of sustainable development goals. The innovation of higher efficiency-domestic LPG burner, which is an important appliance in household and industrial sector (micro, small and medium-size enterprises), help to achieve the 9th Sustainable Development Goal (SDG9). Moreover, with help of CFD, the efficiency of the LPG burners could be further improved. CFD assisted in engineering design maximizes efficient use of resources for design development of the LPG burners. This is related to the 12th Sustainability Development Goal (SDG12).

4. Concluding remarks

In the present study, the CFD simulations were carried out to give a detailed insight into how a swirling flow increased the thermal efficiency of an LPG cooking burner, as previously observed by Tamir et al. [8]. The simulations show that a certain combination of the inclined and the swirl angles generates a swirling central flame, which enhances the turbulence intensity and the entrained secondary air flow rate. These enhancements in turn cause the increase in the combustion temperature and the flow velocity, which significantly improve the net heat flux of the SEB. This leads directly to the enhancement in the heat conversion efficiency and, hence, the thermal efficiency. It is found that the simulated heat conversion efficiency of the SEB is around 3.44% greater than that of the EB. Similarly, the experimental thermal efficiency of the SEB is approximately 2.75% higher than that of the EB. The increment in the heat conversion efficiency obtained by CFD results can be used to predict the increment in the thermal efficiency. This allows the manufacturers to design and optimize the burners more effectively by utilizing the CFD simulations at a much lower cost than the traditional water boiling tests.

CRediT authorship contribution statement

Anirut Matthujak: Supervision, Conceptualization, Methodology, Data curation, Writing – original draft, Funding acquisition. **Mana Wichangarm:** Visualization, Investigation, Validation, Writing – original draft. **Thanarath Sriveerakul:** Supervision, Formal analysis, Writing – review & editing. **Sedthawatt Sucharitpwatskul:** Supervision, Writing – review & editing. **Sutthisak Phongthanapanich:** Supervision, Software.

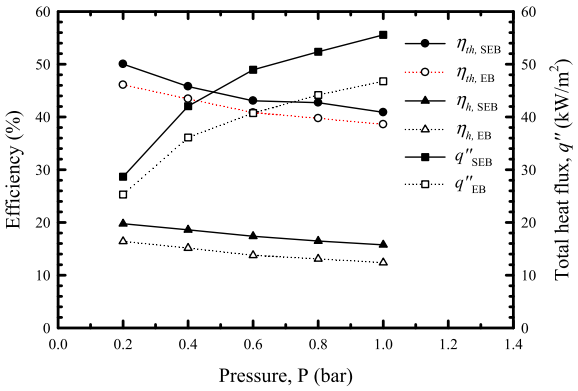

Fig. 8. Effects of the LPG pressure on the net heat fluxes, the heat conversion efficiencies and the thermal efficiencies of the SEB and the EB.

Declaration of competing interest

The authors declare that they have no known competing financial interests or personal relationships that could have appeared to influence the work reported in this paper.

Acknowledgment

This paper is financially supported by Ubon Ratchathani University (Fundamental Fund 2564).

References

[1] A. Matthujak, N. Tidma, A. Yamyuan, Study on Thermal efficiency improvement of energy-saving gas stove by swirling flow, in: Proceedings of the 12th Conference on Energy Network Thailand (ENETT 12), 2016. ENETT12-ET-2. (in Thai).
[2] German Standards and Technical Rules, DIN EN 203-2: Gas-heated Catering equipment, 1997, p. 17.
[3] S. Jugjai, N. Rungsimuntuchart, High efficiency heat-recirculating domestic gas burners, Exp. Therm. Fluid Sci. 26 (5) (2002) 581–592.
[4] A. Datta, M. Das, R. Ganguly, Design, development, and technological advancements in gas burners for domestic cook stoves: a review, Trans. Indian Natl. Acad. Eng. 6 (2021) 569–593.
[5] P. Aroonjarattham, The parametric studied of high pressure gas burner affect thermal efficiency, Eng. J. 20 (3) (2016) 33–48.
[6] A. Chaelek, U.M. Grare, S. Jugjai, Self-aspirating/air-preheating porous medium gas burner, Appl. Therm. Eng. 153 (2019) 181–189.
[7] V. Shtern, A. Borissov, F. Hussain, Temperature distribution in swirling jets, Int. J. Heat Mass Tran. 41 (16) (1998) 2455–2467.
[8] A. Tamir, T. Elperin, S. Yotzer, Performance characteristics of a gas burner with a swirling central flame, Energy 14 (7) (1989) 373–382.
[9] S. Jugjai, S. Tia, W. Trewetasksorn, Thermal efficiency improvement of an LPG gas cooker by a swirling central flame, Int. J. Energy Res. 25 (2001) 657–674.
[10] S.S. Hou, C.Y. Lee, T.H. Lin, Efficiency and emissions of a new domestic gas burner with a swirling flame, Energy Convers. Manag. 48 (2007) 1401–1410.
[11] D. Basu, R. Saha, R. Ganguly, A. Datta, Performance improvement of LPG cook stoves through burner and nozzle modifications, J. Energy Inst. 81 (2008) 218–225.
[12] H.S. Zhen, C.W. Leung, T.T. Wong, Improvement of domestic cooking flames by utilizing swirling flows, Fuel 119 (2014) 153–156.
[13] A. Kotb, H. Saad, Case study for co and counter swirling domestic burner, Case Stud. Therm. Eng. 11 (2018) 98–104.
[14] A.A. Moustafa, H.E. Saad, M. Kamal, The effect of different swirling flow patterns on the performance of a domestic single ring burner, IOSR J. Mech. Civ. Eng. 15 (5) (2018) 50–62. Ver. II.
[15] S.S. Hou, C.H. Chou, Parametric study of high-efficiency and low-emission gas burners, Adv. Mater. Sci. Eng. (2013) 2013, https://doi.org/10.1155/2013/154957.
[16] L. Xi, L. Xu, J. Gao, Z. Zhao, Y. Li, Study on flow and heat transfer performance of X-type truss array cooling channel, Case Stud. Therm. Eng. 26 (2021), 101034.
[17] J. Cho, C. Park, W. Choi, Numerical and experimental study of air containment systems in legacy data centers focusing on thermal performance and air leakage, Case Stud. Therm. Eng. 26 (2021), 101084.
[18] M.S. Gad, Z. He, A.S. EL-Shafay, A.I. EL-Seesy, Combustion characteristics of a diesel engine running with Mandarin essential oil -diesel mixtures and propanol additive under different exhaust gas recirculation: experimental investigation and numerical simulation, Case Stud. Therm. Eng. 26 (2021), 101100.
[19] W. Guan, Z. He, L. Zhang, A.I. EL-Seesy, L. Wen, Q. Zhang, L. Yang, Effect of asymmetric structural characteristics of multi-hole marine diesel injectors on internal cavitation patterns and flow characteristics: a numerical study, Fuel 283 (2021), 119324.
[20] A.A. Hosseini, M. Ghodrat, M. Moghiman, S.H. Pourhoseini, Numerical study of inlet air swirl intensity effect of a Methane-Air Diffusion Flame on its combustion characteristics, Case Stud. Therm. Eng. 18 (2020), 100610.
[21] R.M. El-Zoheiry, A.I. EL-Seesy, A.M.A. Attia, Z. He, H.M. El-Batsh, Combustion and emission characteristics of Jojoba biodiesel-jet A1 mixtures applying a lean premixed pre-vaporized combustion techniques: an experimental investigation, Renew. Energy 162 (2020) 2227–2245.
[22] A.A. Hussain, B. Freegh, B.S. Khalaf, H. Towsyfyan, Numerical investigation of heat transfer enhancement in plate-fin heat sinks: effect of flow direction and fillet profile, Case Stud. Therm. Eng. 13 (2019), 100388.
[23] Y. Zhang, C. Ke, Y. Gao, S. Liu, Y. Pan, N. Zhou, Y. Wang, L. Fan, P. Peng, B. Li, R. Ruan, Syngas production from microwave-assisted air gasification of biomass: Part 2 model validation, Renew. Energy 140 (2019) 625–632.
[24] S. Karyeyen, M. Ilbas, Experimental and numerical analysis of turbulent premixed combustion of low calorific value coal gases in a generated premixed burner, Fuel 220 (2018) 586–598.
[25] P. Boggavarapu, B. Ray, R.V. Ravikrishna, Thermal Efficiency of LPG and PNG-fired burners: experimental and numerical studies, Fuel 116 (2014) 709–715.
[26] J.C. Francisco, Y. Cadavid, A.A. Amell, A.E. Arrieta, J.D. Echavarría, Numerical and experimental methodology to measure the thermal efficiency of pots on electrical stoves, Energy 73 (2014) 258–263.
[27] M. Wichangarm, A. Matthujak, T. Sriveerakul, S. Sucharitpwatskul, S. Phongthanapanich, Numerically study of combustion phenomena in the energy-saving cooking stove, in: Proceeding of the 9th TSME International Conference on Mechanical Engineering vol. 2018, 2018, pp. 46–51.

[28] A. Mustafa, N.S. Nasri, Computational studies of fuel and air mixing characteristics of a low pressure domestic gas appliance, in: Proceeding of the International Conference on Chemical and Bioprocess Engineering, University Malaysia Sabah, Kota Kinabalu, Malaysia, 2003.
[29] N. Piyaprai, T. Sriveerakul, M. Wichangarm, A. Namkhat, CFD simulation for air-fuel gas mixing flow in mixing tube of a KB-5 cooking burner, in: Proceeding of the 27th Conference on Mechanical Engineering Network Thailand, ME-NETT 27), 2013 (in Thai).
[30] W. Treedet, R. Suntivarakorn, Effect of various inlet geometries on swirling flow in can combustor, J. Mech. Eng. Sci. 12 (2) (2018) 3712–3723.
[31] S.E. Hosseini, G. Bagheri, M.A. Wahid, Numerical investigation of biogas flameless combustion, Energy Convers. Manag. 81 (2014) 41–50.
[32] Y. Li, R. Li, D. Li, J. Bao, P. Zhang, Combustion characteristics of a slotted swirl combustor: an experimental test and numerical validation, Int. Commun. Heat Mass Tran. 66 (2015) 140–147.
[33] A. Namkhat, S. Jugjai, Primary air entrainment characteristics for a self-aspirating burner: model and experiments, Energy 35 (4) (2010) 1701–1708.
[34] United Nations, Transforming Our World: the 2030 Agenda for Sustainable Development, UN Publishing, New York, 2015.